PHYSICAL REVIEW B VOLUME 35, NUMBER 16 1 JUNE 1987

Dynamics of strongly coupled model rotational-translational systems

S. D. Mahanti and G. Zhang
Department of Physics and Astronomy, Michigan State University, East Lansing, Michigan 48824
and Center for Fundamental Materials Research, Michigan State University, East Lansing, Michigan 48824

G. Kemeny
Department of Natural Science, Michigan State University, East Lansing, Michigan 48824
and Department of Physics and Astronomy, Michigan State University, East Lansing, Michigan 48824
(Received 14 November 1986)

The power spectra of different dynamic correlation functions of a single one-dimensional rotor coupled to a bath of harmonic oscillators have been studied using molecular dynamics and, to some extent, Mori theory. The latter results, obtained in the lowest nontrivial order of approximation, are found to be unreliable over most of the parameter range studied. The molecular dynamics results are compared both to experiment and to our earlier results for the one-dimensional oscillator which is an example of a linear system. We find that the present nonlinear system retains some of the general spectral features of the linear one. However, the nonlinear coupling strongly affects the low-frequency end of the velocity power spectrum $P_v(\omega)$, particularly in the strong-coupling limit $\alpha \to 1$. The weak divergence in $P_v(\omega)$ as $\omega \to 0$ for $\alpha = 1$ present in the oscillator case is absent in the rotor system. For nonzero α $(0 < \alpha < 1)$ we find that, for temperatures smaller than the adiabatic barrier height, the qualitative structure of the sine and the cosine power spectral functions are relatively insensitive to α. The velocity power spectrum, however, is strongly α dependent and can in principle distinguish between the strong $(\alpha \to 1)$- and weak $(\alpha \to 0)$-coupling regimes.

I. INTRODUCTION

In the dynamical study of rotation-translation coupling, even the case of a single rotating molecule coupled to a vibrating lattice is not well understood, especially when the coupling is strong. Systems of this type are molecular impurities, e.g., CN^- and O_2^- in alkali halide crystals at very low concentrations,[1] or O_2 and N_2 molecules on a graphite surface at very low concentrations surrounded by a two-dimensional (2D) Ar matrix.[2] In such systems the coupling mentioned above may be quite strong. The rigid-lattice potential well for the rotation may combine with the translation-rotation coupling to produce a shallow effective potential. This was suggested to us by the example of CN^- impurities in KBr. Theoretical estimates for a rigid crystal led to a barrier height of several hundred K,[1,3] while the experimental results gave about 50 K.[4,5] It is physically obvious that if properly synchronized, the neighboring ions can get out of the way of the rotating molecule, thereby reducing the height of the effective barrier.[6]

In our initial attempt[1,7] at solving this problem we took the coupled translation-rotation Hamiltonian appropriate for a CN^- impurity in KBr and followed the Mori-theory approach of de Raedt and de Raedt,[8] and of de Raedt and Michel[9] to calculate the dynamic correlation functions for different rotational variables, keeping only second and fourth moments of these variables (higher moments are approximated in terms of these two and zeroth-order moments). To this order of approximation, the translational motion of the surrounding lattice is taken into account only in an average way, so that the vibrational dynamics is not adequately considered. We found,[1] to our surprise, that for CN^- in KBr, in the parameter regime in which the barrier height came out reasonably, the Raman spectrum for both the E_g and T_{2g} symmetries had a dominant central peak. This contradicted the experimental results,[5] which gave a central peak for one symmetry and a finite-frequency peak for the other. On the other hand, the calculation of de Raedt and Michel,[10] which only considers a rigid barrier, gives only one central peak, but at the cost of having to adjust the rigid potential barrier to the experimental height and neglecting the rotation-translation coupling, which is known to be strong in these systems. The disagreement between our calculation and experiment may be either due to the inadequacy of the model Hamiltonian or to the approximation scheme used in the Mori theory. We have therefore reexamined the approximation scheme and found it to be ambiguous.

Lacking a trustworthy approximation scheme, we decided to choose the simplest possible model which contains all the essentials of the translation-rotation coupling (the "hydrogen atom" of this problem) and to solve it exactly numerically and also to compare this result with that of the de Raedt[7] scheme of Mori theory, and with another scheme we devised.[11] Our model leads to a generalized Langevin equation, in which a one-dimensional rotor is coupled to Debye oscillators of one, two, and three dimensions. It, therefore, is different from the work of Gerling and de Raedt,[12] which concerns a two-dimensional rotor whose coupling to translations is neglected; it is subject to random potential fluctuations

from a thermal bath and frequency-independent damping. This work, therefore, leads to an ordinary, rather than a generalized, Langevin equation. Also, they calculate time-dependent correlation functions, rather than their Fourier transforms, and comparison with our results is not possible.

A matter of particular interest for us is what we call the strong-coupling limit. For a certain value of the translation-rotation coupling parameter the effective potential well vanishes. This, however, does not mean that the rigid potential and the translation-rotation interactions do not have a residual dynamical effect. These terms cancel each other in the rotational equation of motion only in the adiabatic limit, i.e., for a rotor of zero angular velocity.

We have earlier solved a linear version of this problem in which the rotor itself is replaced by an oscillator.[13] One advantage of the oscillator problem is that it can be solved analytically as well as numerically. A comparison of the solution of the rotor and oscillator problems allows us to assess the effect of nonlinearity on several fundamental properties such as the nature of the dynamic response, approach to thermodynamic equilibrium, etc.

The outline of this paper is as follows: In Sec. II we introduce the model Hamiltonian, transform to dimensionless variables, and describe the equations of motion in two forms: the coupled rotor and oscillator differential equations, and the integro-differential equation for the rotor from which the oscillators have been eliminated, except for initial conditions, i.e., the generalized Langevin equation. In Sec. III we describe two Mori-theory approximation schemes. In Sec. IV we give the molecular-dynamics results for a system with 100 or 1000 oscillators (and, as always, a single rotor), for various dimensionless values of the coupling parameter, rotor moment of inertia, and temperature. These are the only three numerical parameters in the system after dimensionless parameters have been introduced. In addition, there is the parameter of the bath dimensionality (bath density of states). In Sec. V we consider systems with only 10 oscillators to analyze the origin of zeros in the spectral functions of certain rotational variables. In Sec. VI we compare the rotor results with those for an oscillator. Section VII is a comparison with the Mori-theory results and Sec. VIII with experiment.

II. THE MODEL

The Hamiltonian of the translation-rotation coupling model is chosen[14] as

$$H=\tfrac{1}{2}I\dot{\theta}^2-D\cos\theta + \sum_{i=1}^{N}\left[\tfrac{1}{2}M_i\dot{x}_i^2+\tfrac{1}{2}k_i x_i^2-A_i/\sqrt{N}\,x_i\sin(\theta/2)\right] . \quad (2.1)$$

Here, θ is the rotor or pendulum angle and the x_i's are the coordinates of the N oscillators. The interaction is such that the displaced harmonic-oscillator approximation yields a potential-energy term of the form $\cos\theta$ and thus may partially or totally cancel the rigid potential (we assume $D>0$). We assume, for sake of simplifying the equations of motion, that A_i^2/K_i are independent of i and introduce

$$W_A=\frac{1}{N}\sum_{i=1}^{N}A_i^2/4K_i . \quad (2.2)$$

Using this quantity we define the dimensionless coupling constant $\alpha=W_A/D$. The dimensionless time is $\tau=\omega_D t$, where ω_D is the Debye frequency of the oscillators. We also define the dimensionless uncoupled oscillator frequencies $\Omega_i=\omega_i/\omega_D$, dimensionless oscillator coordinates $X_i=\sqrt{M_i}/D\omega_D x_i$, velocities $\dot{X}_i=dX_i/d\tau$, and moment of inertia for the rotor $\mu=I\omega_D^2/D$. In terms of these dimensionless quantities, the equations of motion can be written as

$$\mu\ddot{\theta}+\sin\theta-\sqrt{\alpha/N}\sum_i\Omega_i X_i\cos(\theta/2)=0 \quad (2.3)$$

and

$$\ddot{X}_i+\Omega_i^2X_i-2\sqrt{\alpha/N}\,\Omega_i\sin(\theta/2)=0 . \quad (2.4)$$

In the molecular-dynamics calculations we solve Eqs. (2.3) and (2.4) with a harmonic-oscillator density of states which, in the continuum limit, corresponds to the n-dimensional Debye density of states $\rho_n(\Omega)$, where

$$\rho_n(\Omega)=n\Omega^{n-1},\quad n=1,2,3 \text{ and } 0<\Omega\le 1 . \quad (2.5)$$

The harmonic-oscillator equations can be solved analytically and the solution substituted into Eq. (2.3), leading to the integro-differential equation

$$\mu\ddot{\theta}+\sin[\theta(\tau)]-2\alpha\cos[\theta(\tau)/2]\int_0^\tau K(\tau-\tau')\sin[\theta(\tau')/2]d\tau' -\sqrt{\alpha/N}\cos[\theta(\tau)/2]\sum_i[\Omega_i X_i(0)\cos(\Omega_i\tau)+\dot{X}_i(0)\sin(\Omega_i\tau)]=0 , \quad (2.6)$$

where, in the $N\to\infty$ limit,

$$K(\tau)=n\int_0^1 d\Omega\,\Omega^n\sin(\Omega\tau) . \quad (2.7)$$

The initial values for the oscillator coordinates and velocities are chosen from a thermal bath of dimensionless temperature, $T^*=k_BT/D$, and the initial rotor coordinate and velocity are chosen zero. With this choice of initial conditions for the rotor, the oscillators initially have zero interaction energy with the rotor, making the assignment of initial oscillator energies unique. This also simplifies the following equation. Integrating the third term in Eq. (2.6) by parts leads to the generalized nonlinear Langevin equation

$$\mu\ddot{\theta}+(1-\alpha)\sin[\theta(\tau)]+\alpha\cos[\theta(\tau)/2]\int_0^\tau H(\tau-\tau')\cos[\theta(\tau')/2]\dot{\theta}(\tau')d\tau'-\sqrt{\alpha}\cos[\theta(\tau)/2]F(\tau)=0 , \quad (2.8)$$

where

$$F(\tau)=\frac{1}{\sqrt{N}}\sum_i [\Omega_i X_i(0)\cos(\Omega_i\tau)+\dot{X}_i(0)\sin(\Omega_i\tau)] , \tag{2.9}$$

and

$$H(\tau)=n\int_0^1 d\Omega\,\Omega^{n-1}\cos(\Omega\tau) . \tag{2.10}$$

In Eq. (2.8) the rigid force term is renormalized to $(1-\alpha)\sin\theta$. Thus $\alpha=1$, our strong-coupling limit, corresponds to a "free" rotor, which is still coupled to its own past via the velocity-dependent term, and to the initial conditions of the bath oscillators in the last term (random-force term).

III. MORI THEORY

In studying the dynamics of molecules in solids, the Mori theory[1,7–10] is frequently used. In this theory one calculates the relaxation function associated with the dynamic variable of interest using a continued-fraction scheme. The continued fraction has to be broken at some stage (except for the few cases where an exact solution is possible) and a suitable approximation to the memory function has to be made at this stage. In a scheme due to de Raedt and de Raedt,[8] and to de Raedt and Michel,[9] one introduces a set of orthogonalized dynamical variables,

$$A_1=LA_0 , \tag{3.1}$$

$$A_n=LA_{n-1}-\Delta_{n-1}^2 A_{n-2} , \tag{3.2}$$

where L is the Liouville operator and the Δ_n's are given by the ratios of moments (A_n,A_n), i.e.,

$$\Delta_n^2=(A_n,A_n)/(A_{n-1},A_{n-1}) . \tag{3.3}$$

The relaxation function for the variable A is then given by

$$\Phi_{00}(z)=\cfrac{(A_0,A_0)}{z-\cfrac{\Delta_1^2}{z-\cdots\cfrac{\Delta_n^2}{z+\Sigma_{nn}(z)}}} . \tag{3.4}$$

Here, $\Sigma_{nn}(z)$ is the memory function and in Ref. 9 it is approximated as

$$\Sigma_{nn}(z)=-\frac{\Delta_{n+1}^2}{z+i(\Delta_n^2+\Delta_{n-1}^2)^{1/2}} . \tag{3.5}$$

Evaluation of $\Phi_{00}(z)$ at $z=0$ for odd and even orders of the approximation scheme, respectively, yields

$$\Phi_{00}(0)=i(A_0,A_0)\frac{\Delta_2^2}{\Delta_1^2}\cdots\frac{\Delta_{2m}^2}{\Delta_{2m-1}^2}\frac{1}{(\Delta_{2m-1}^2+\Delta_{2m}^2)^{1/2}} , \quad n=2m+1 \tag{3.6}$$

and

$$\Phi_{00}(0)=i(A_0,A_0)\frac{\Delta_2^2}{\Delta_1^2}\cdots\frac{(\Delta_{2m}^2+\Delta_{2m+1}^2)^{1/2}}{\Delta_{2m+1}^2} , \quad n=2m . \tag{3.7}$$

If one now assumes that the ratio of Δ_n's converges to unity, although this is, in general, not assured, i.e., that

$$\frac{\Delta_{2m+1}^2}{\Delta_{2m}^2}\to 1, \quad m\to\infty \tag{3.8}$$

then one finds that the ratio of even- to odd-order $\Phi_{00}(0)$'s goes to 2. Thus the relaxation function oscillates with the order of the approximation. This circumstance suggested to us that the approximation scheme may not be unique and that different ways of determining the memory function may exist.

The above approximation scheme exhibited in the lowest sensible order makes use of the projection operators P and Q, where P projects onto the subset of variables A_0 and A_1, while Q projects onto A_2, A_3, etc. The operator that occurs in the memory function is

$$B=QLQLA_2=QL^4A_0-\frac{(L^2A_0,L^2A_0)}{(A_1,A_1)}A_2 . \tag{3.9}$$

The approximation scheme now replaces the first term on the right-hand side by an imaginary number, this number being determined by the coefficient of A_2 in the second term. An alternative way of writing the last equation is

$$B=A_4+(\Delta_1^2+\Delta_2^2+\Delta_3^2)A_2-(\Delta_1^2+\Delta_2^2)A_2 , \tag{3.10}$$

where the last term on the right-hand side contains the imaginary number that replaces the first two terms. This latter form of the equation shows that there are an infinite number of ways in which B can be written as a sum. There is no unique choice, but a plausible one is

$$B=QL^2A_2-QLPLA_2 , \tag{3.11}$$

which can also be written as

$$B=A_4+(\Delta_2^2+\Delta_3^2)A_2-\Delta_2^2A_2 . \tag{3.12}$$

Again, the last term contains the imaginary number that replaces the first two. The results for the memory function in the two schemes are

$$\Sigma_{11}^{\mathrm{RM}}(z)=\frac{\Delta_2^2}{z+i(\Delta_1^2+\Delta_2^2)^{1/2}}$$

and

$$\Sigma_{11}^{\mathrm{MK}}(z)=\frac{\Delta_2^2}{z+i\Delta_2} , \tag{3.13}$$

where the first one is the result of the de Raedt–Michel[9] scheme and the second one is ours.[11] In the second scheme there is no problem with the factor of 2 and the width is determined by the last Δ_n alone instead of the last two.

We have shown in earlier papers[1,7] that the spectral distribution for the relaxation function (normalized to unity) in this order can be written in the form

$$\tilde{S}(\bar{\omega})=\frac{1}{\pi}\left[\frac{A\Gamma}{\bar{\omega}^2+\Gamma^2}+\frac{1}{2}\left[\frac{X\gamma-Y(\bar{\omega}+\delta)}{(\bar{\omega}+\delta)^2+\gamma^2}+\frac{X\gamma+Y(\bar{\omega}-\delta)}{(\bar{\omega}-\delta)^2+\gamma^2}\right]\right] , \tag{3.14}$$

where the parameters $A,\Gamma,X,Y,\gamma,\delta$ are functions of R, and where

$$R=\langle\omega^4\rangle^{1/2}/\langle\omega^2\rangle \text{ and } \bar{\omega}=\omega/\langle\omega^2\rangle^{1/2}, \quad (3.15)$$

$\langle\omega^n\rangle$ being the nth moment of the spectral function which can be calculated exactly. If these approximation schemes are applied to the relaxation function of coordinate of an harmonic oscillator with the coupling of this oscillator to some external system going to zero, then the first scheme leads to $A\to 0$, $\Gamma\to 1$, while the second scheme leads to $A\to 0$, $\Gamma\to 0$. Utilizing Schwinger's[15] exact treatment of the Brownian motion of a quantum oscillator, we find that the second result is compatible with it, but the first is not. When the coupling goes to zero, both the amplitude and the width of the central peak should go to zero, not just the amplitude. The detailed differences can be seen in Fig. 1, where (a) refers to the first scheme (RM) and (b) to the second (MK). The quantitative behavior of all parameters is changed between the two approximation schemes. It is to be kept in mind that the weight of the central peak is $A=1-X$.

We shall apply both the approximation schemes to the Hamiltonian of Eq. (2.1), with the dynamical variable A_0 chosen in three different ways:

$$A_0=\sin(\theta/2),\quad A_0=\cos(\theta/2),\quad A_0=\dot{\theta}\ . \quad (3.16)$$

The results for the two parameters which occur in the relaxation functions are given in Table I for general values of the coupling strength α, for $\omega_0^2=(\langle\omega^2\rangle/\omega_D^2)$, which are the second moments in Debye-frequency units, and the dimensionless quantity R, which has been defined in Eq. (3.15). In Table II these values are given specifically for the strong-coupling limit $\alpha=1$. The spectral representation of a particular relaxation function in the dimensionless units introduced for the Hamiltonian can be written in the form

$$S(\Omega)=\frac{(A_0,A_0)}{\pi}\frac{B}{(\Omega-A)^2+B^2}\ , \quad (3.17)$$

where

$$A=\frac{\langle\Omega^2\rangle[\Omega-\Sigma'(\Omega)]}{[\Omega-\Sigma'(\Omega)]^2+[\Sigma''(\Omega)]^2}\ , \quad (3.18)$$

$$B=\frac{\langle\Omega^2\rangle[\Sigma''(\Omega)]^2}{[\Omega-\Sigma'(\Omega)]^2+[\Sigma''(\Omega)]^2}\ . \quad (3.19)$$

Here, $\langle\Omega^2\rangle$ is the average value of Ω^2 over the Debye spectrum, and the real and the imaginary parts of the complex self-energy $\Sigma(\Omega)=\Sigma'(\Omega)-i\Sigma''(\Omega)$ can be obtained from the following two expressions for $\Sigma(\Omega)$:

$$\Sigma(\Omega)=\langle\Omega^2\rangle\frac{R^2-1}{\Omega+iR(\langle\Omega^2\rangle)^{1/2}} \quad (3.20)$$

in the first scheme (RM), and

$$\Sigma(\Omega)=\langle\Omega^2\rangle\frac{R^2-1}{\Omega+i[(R^2-1)\langle\Omega^2\rangle]^{1/2}} \quad (3.21)$$

in the second (MK).

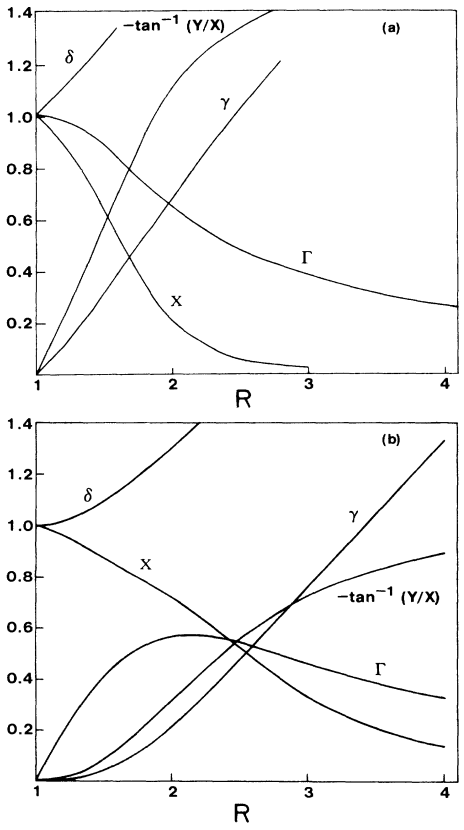

FIG. 1. Parameters of the (a) first (RM) and (b) second (MK) schemes of the Mori theory.

IV. MOLECULAR DYNAMICS

The dimensionless equations of motion (2.3) and (2.4) were solved for different values of the parameters α, μ, and T. One Debye period was subdivided into 64 time steps and 128 periods were run. Our experience has been that transients usually play no role in the results and therefore no parts of the MD runs have been discarded. The thermal bath was represented by 1000 oscillators (occasionally by 100) and an ensemble of 100 systems were averaged over. The initial thermal energy was distributed among all the oscillators. The rotor was invariably started with $\theta=0$ and $\dot{\theta}=0$, so the rotor has no kinetic or coupling energy and its potential energy was at a minimum. In most of the calculations, the bath density of states was chosen to be 2D Debye [$n=2$ in Eq. (2.5)], but we have, for comparison, taken also 1D and 3D densities of states on occasion. The quantities calculated are the power spectra of the rotor velocity $\dot{\theta}$, $\sin(\theta/2)$, and $\cos(\theta/2)$. The latter two, respectively, correspond to the E_g and T_{2g} symmetries in a cubic crystal-field potential when the potential minima are along the [111] direction and its equivalent directions. In the central oscillator case, where the rotor itself is replaced by a harmonic oscillator,[13] we calculated only the power spectrum of the velocity. We note that the power spectra of different time derivatives of the coordinate do not yield substantially new information because they are related simply by powers of the frequency. The sine and cosine functions there are meaningless,

TABLE I. The spectral parameters of Mori theory, $\omega_0^2=\langle\omega^2\rangle/\omega_D^2$ and R [see Eq. (3.15)], for the relaxation functions of the three dynamic variables. T^*, μ, and α are, respectively, temperature, moment of inertia, and coupling constant, all dimensionless.

	ω_0^2	R^2
$\sin(\theta/2)$	$\frac{T^*}{4\mu}\frac{\langle\cos^2(\theta/2)\rangle}{\langle\sin^2(\theta/2)\rangle}$	$\frac{\langle\sin^2(\theta/2)\rangle}{\langle\cos^2(\theta/2)\rangle^2}\left[\frac{1}{2}\langle 3-\cos\theta\rangle+\frac{1-\alpha}{T^*}\langle -1+2\cos\theta+3\cos^2\theta\rangle+\frac{\alpha}{T^*}\langle(1+\cos\theta)^2\rangle\right]$
$\cos(\theta/2)$	$\frac{T^*}{4\mu}\frac{\langle\sin^2(\theta/2)\rangle}{\langle\cos^2(\theta/2)\rangle}$	$\frac{\langle\cos^2(\theta/2)\rangle}{\langle\sin^2(\theta/2)\rangle^2}\left[\frac{1}{2}\langle 3+\cos\theta\rangle+\frac{1-\alpha}{T^*}\langle 1+2\cos\theta-3\cos^2\theta\rangle+\frac{\alpha}{T^*}\langle\sin^2\theta\rangle\right]$
$\dot\theta$	$\frac{1}{\mu}\langle\cos\theta+\alpha\sin^2(\theta/2)\rangle$	$\left[(1-\alpha\langle\cos^2\theta\rangle+\alpha\langle\cos\theta\rangle+\alpha^2\langle\sin^4(\theta/2)\rangle+\frac{\alpha T^*}{4}\langle\sin^2(\theta/2)\rangle+\alpha\mu\langle\Omega^2\rangle\langle\cos^2(\theta/2)\rangle\right]/\langle\cos\theta+\alpha\sin^2(\theta/2)\rangle^2$

thus making the rotor problem much richer. It is also not obvious that for the rotor problem which quantity, the power spectrum of the velocity or the sine, or both, should be the analogue of the velocity for the oscillator (see discussions below).

A. Strong-coupling limit ($\alpha=1$)

In Fig. 2 we exhibit the results for the parameter values $\alpha=1$, $\mu=1$, and $T=1$ for the 2D density of states ($n=2$). The velocity-power spectrum P_v shows a broad central peak and another broad peak somewhat below the Debye frequency of unity. The sine-power spectrum has a dominating low-, but not zero-, frequency narrow peak, and another weak and broad one above unity. The cosine power spectrum has also a low-frequency peak, although not as low as the sine one, but it has no high-frequency peak. In comparison with Fig. 2, Fig. 3 shows the role of dimensionality of the bath. As for the $n=2$ case, P_v can be represented by two broad peaks for $n=1,3$, although for $n=1$ the central peak is difficult to extract visually. The high-frequency peak shifts towards lower frequency with decreasing dimensionality ($\Omega_{\max}\simeq 1, 0.9, 0.6$ for $n=3,2,1$, respectively). The central peak, particularly its shape and width, are dimension sensitive, the latter increasing with n. For $n=1,2$ all the peaks are nearly Gaussian, but the central peak for $n=3$ deviates considerably from a Gaussian shape. Furthermore, the central-peak weight increases with n, dominating the velocity-power spectrum for the 3D density of states. The sine and cosine both have central peaks in one dimension, the first one narrow and the latter broad, while in three dimensions the low-frequency peaks are more decisively noncentral than for two dimensions. For the above set of parameters and two dimensions, we have also carried out calculations at different temperatures. The effect of in-

TABLE II. Same as Table I, but with $\alpha=1$.

	ω^2	R^2
$\sin(\theta/2)$	$T^*/4\mu$	$\frac{3}{2}(1+1/T^*)$
$\cos(\theta/2)$	$T^*/4\mu$	$3(1+1/3T^*)$
$\dot\theta$	$T^*/2\mu$	$\frac{3}{2}(1+T^*/2+\frac{4}{3}\mu\langle\Omega^2\rangle)$

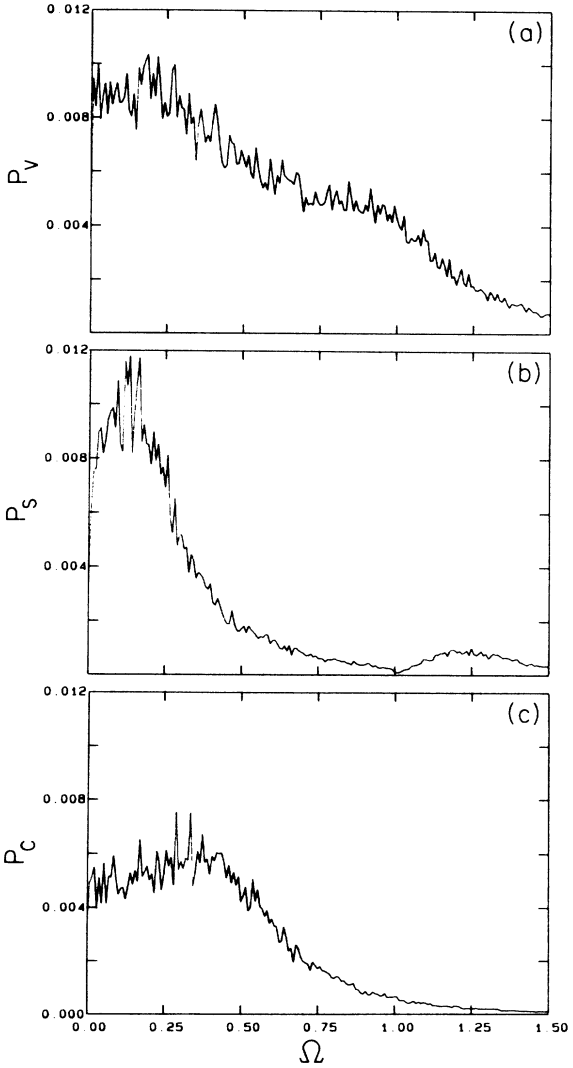

FIG. 2. Power spectra (in arbitrary units) for (a) $\dot\theta$, (b) $\sin(\theta/2)$, and (c) $\cos(\theta/2)$ of a rotor with $\alpha=1$, $\mu=1$, and $T^*=1$, with a 2D Debye density of 1000 oscillators.

creasing temperature in the "free-rotor" ($\alpha=1$) limit is basically to broaden the spectrum with little or no spectral weight shifting from one peak to the other. There is also hardly any thermal shift of the peak positions.

Figure 4, together with Fig. 2, offers a comparison of the effect of the moment of inertia (μ) in two dimensions, again in the strong-coupling limit with the smaller one ($\mu=0.5$) on the left. Comparing the frequency dependence of $P_v(\Omega)$ for $\mu=0.5$, 1, and 2, we see two characteristic features. The high-frequency peak shifts towards a lower frequency with increasing μ. The structure in the lower-frequency region is quite unusual for $\mu=0.5$; there is apparently no central peak which is seen for $\mu=1,2$. The power spectrum can be approximated by two finite-frequency peaks and possibly a very weak central peak. The low-frequency peak in P_s, which dominates the power spectrum for all values of Ω, moves to lower frequencies with increasing μ. The cosine power spectrum for $\mu=0.5$ resolves into two peaks, one of them central. The other peak moves to higher frequencies, as compared to the higher-μ cases, thereby revealing the hitherto hidden central peak.

B. Intermediate- and weak-coupling limit ($\alpha<0.5$)

Figure 5 shows a comparison of two cases in which the temperatures T are taken equal to half the barrier heights of the adiabatic potential $2(1-\alpha)$ for two different values of the coupling constant but with the same μ ($=1$). Comparing with Fig. 2, we see that the high-frequency peak structure in both P_v and P_s became much more pronounced, representing a well-developed librational motion. In addition, the broad low-frequency peak in P_s shifts toward higher frequency with decreasing α. The cosines' low-frequency peaks have become central. The differences between the two cases in question are only quantitative.

It turns out that, for most of the diatomic impurities studied experimentally, $\mu\gg1$. Therefore, to understand

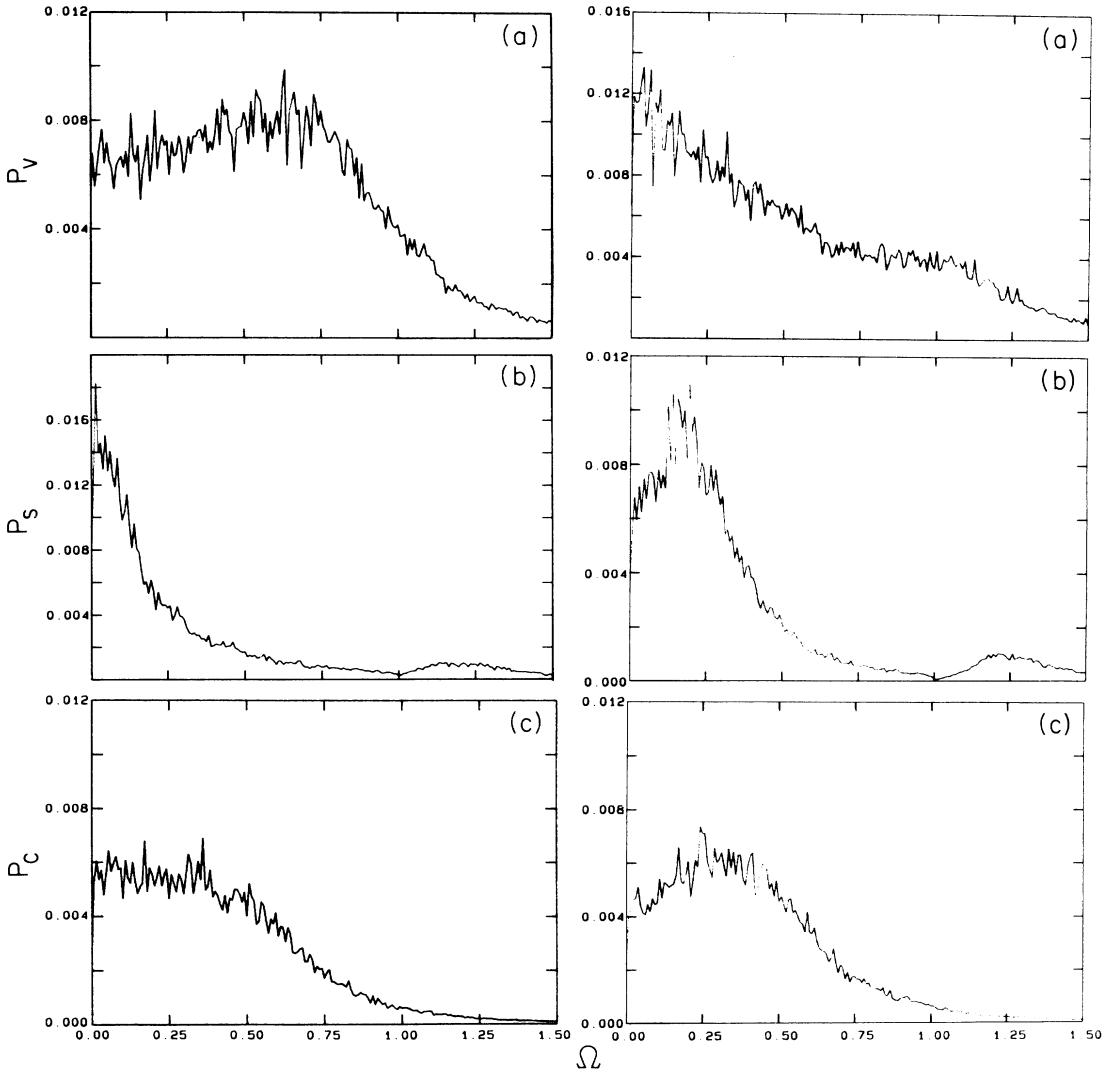

FIG. 3. Same as Fig. 2, except for 1D (left-hand panel) and 3D (right-hand panel) Debye densities of states.

the spectral properties of these heavy impurities we have run molecular-dynamics simulations for a system with $\mu=4$, $\alpha=0.25$, $n=2$, and $T=0.25$, 0.75, 3.0, and 6.0, and results for $T=0.75$ and 3.0 are given in Fig. 6. In contrast to the $\mu=1$ case, we see only one broad resonance structure in P_s whose shape is strongly T dependent. P_v, on the other hand, has one peak (broadened librational motion) at $T=0.25$, not shown in the figure, which is a factor of 6 smaller than the adiabatic barrier height $[2(1-\alpha)=1.5]$. With increasing T, P_v develops a distinct two-peak structure [Fig. 6(a)], the central peak coming from the over-the-barrier motion. Finally, at very high T ($T=3.0,6.0$) only the central peak remains and its width decreases with increasing T. P_c, which is dominated by a slightly broadened (perhaps exponential T dependence) central peak at low T, develops a broad finite-frequency peak at high T [Fig. 6(c)]. One interesting feature of our model is that even at temperatures 3 times larger than the barrier height, P_s and P_c show very different dynamic response.

V. ROTOR COUPLED TO SMALL NUMBER OF OSCILLATORS ($N=10$)

Looking at $P_s(\Omega)$ we find that $P_s(1)=0$ for all values of α,μ,T within numerically accuracy. To explore the origin of this behavior, we have looked at a system of one rotor coupled to a bath of 10 oscillators. Figure 7 shows the sine power spectrum for this case for $\alpha=\mu=T=1$. The bath oscillator frequencies have been chosen as $(I/10)^{12}$, $I=1,10$. Note that at the bare bath frequencies the sine power spectrum vanishes. By Fourier-transforming (FT) Eq. (2.4), we find

$$X_i(\Omega)=2\left[\frac{\alpha}{N}\right]^{1/2}\Omega_i\frac{S(\Omega)}{\Omega_i^2-\Omega^2}\ , \tag{5.1}$$

where $S(\Omega)$ is the FT of $\sin(\theta/2)$. Since $X_i(\Omega)$ must be finite for all Ω, it follows that $S(\Omega_i)=0$. As the number of oscillators increases and their frequency separations decrease, the molecular-dynamics calculation smooths out

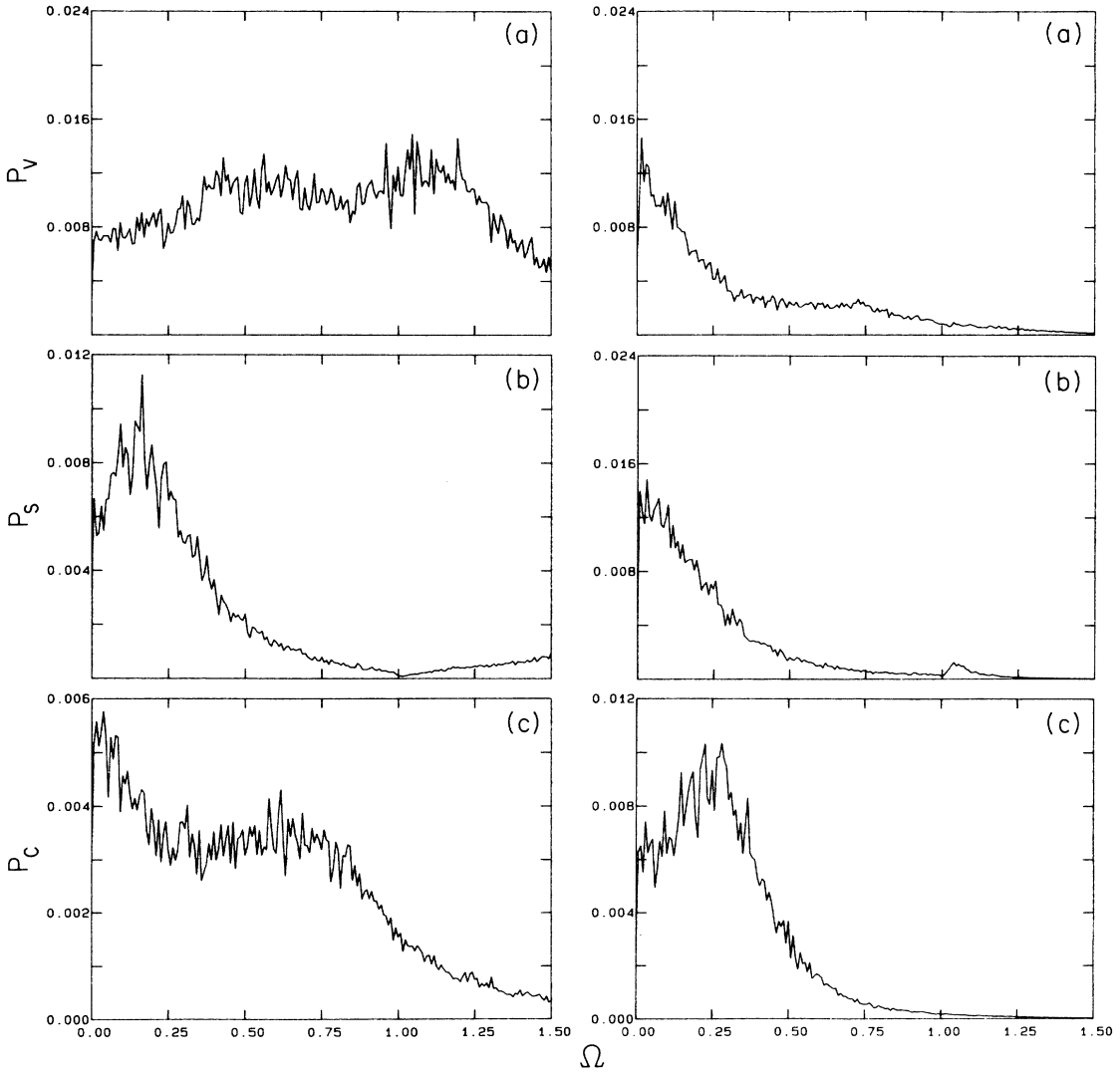

FIG. 4. Same as Fig. 2, except for $\mu=0.5$ (left-hand panel) and $\mu=2.0$ (right-hand panel).

the spectrum, but at $\Omega=1$, where the bath-frequency spectrum terminates, it quite successfully approximates zero. In the case of a central oscillator, Eq. (5.1) should be replaced by

$$X_i(\Omega)=\left[\frac{\alpha}{N}\right]^{1/2}\Omega_i\frac{\theta(\Omega)}{\Omega_i^2-\Omega^2}\ . \tag{5.2}$$

Since the Fourier transforms of θ and $\dot{\theta}$ only differ in a factor of $i\Omega$, it is obvious that the velocity-power spectrum for the oscillator should show some resemblance to the sine-power spectrum of the rotor.

VI. COMPARISON WITH CENTRAL OSCILLATOR

Comparing our present results with those of our earlier paper[13] in which the rotor itself is replaced by an oscillator, we find that the power spectrum of the sine in this work resembles that of the velocity in the earlier one, verifying the expectation at the end of the preceding section. Since the oscillator is a linear system, the power spectrum splits into two disconnected pieces, a continuous one in the region $0\leq\Omega\leq1$ and a δ-function one above at $\Omega\geq1$. In order to gain physical insight, let us examine the oscillator results for the weak coupling $\alpha=0.1$, and small ($\mu=0.5$) and large ($\mu=2$) mass. In the former case the velocity-power spectrum has most of its weight at the pole ($\Omega>1$, bound state), while in the latter virtually all of it lies in the continuum ($\Omega<1$, resonance). Stronger coupling tends to obscure these characteristics, both aspects being present for both values of μ. For $\mu=1$, where the uncoupled oscillator frequency coincides with the Debye frequency, both aspects are present for all values of the coupling constant used. Reviewing now all the figures (Figs. 2–6) of this paper for the sines, we note that they have their high-frequency peaks above unity, where all the oscillator peaks were. The low-frequency peaks are all at frequencies between 0 and 1. This again agrees with the

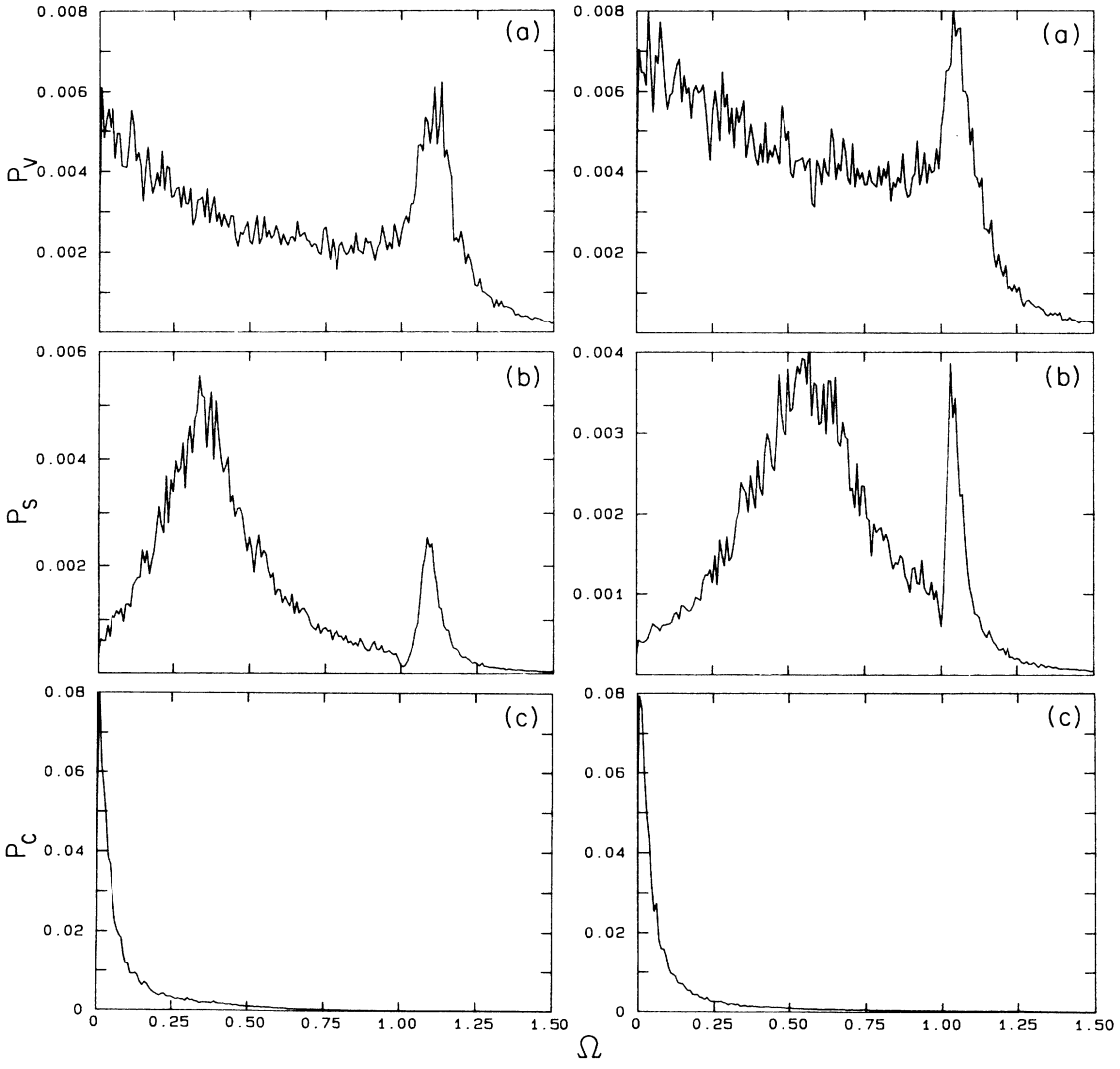

FIG. 5. Same as Fig. 2, except $\alpha=0.5$, $T^*=0.5$ (left-hand panel) and $\alpha=0.25$, $T^*=0.75$ (right-hand panel).

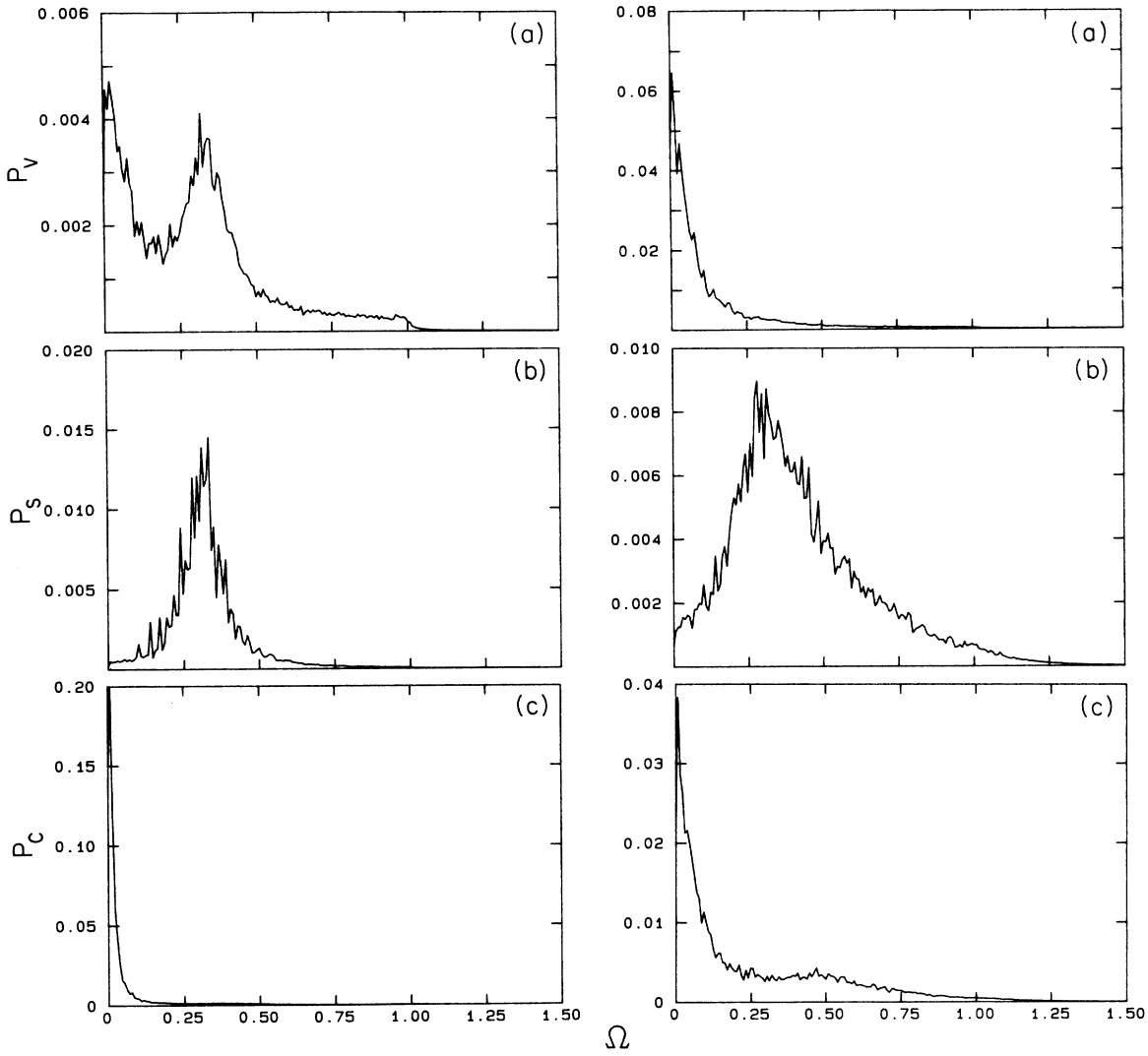

FIG. 6. Same as Fig. 2, except for $\alpha=0.25$, $\mu=4.0$, and $N=100$ oscillators, with $T^*=0.75$ (left-hand panel) and $T^*=3.0$ (right-hand panel).

oscillator case with the exception of $\alpha=1$, for which the oscillator peak is at zero frequency. The position of the high-frequency peak of the rotor shifts to higher frequencies with increasing α and decreases with increasing μ, the way the pole frequency for the oscillator depends on these parameters. We therefore conclude that the rotor itself can to some extent be described as an oscillator even for temperatures as high as half the adiabatic potential barrier height as far as the sine power spectrum is concerned. The analogy is not perfect, because both the dynamics and the dynamical variable in question are periodic functions of θ, which is not the case for the oscillator. The peaks in the velocity spectrum are not easily identifiable with those of the sine. The velocity is not a periodic function of θ, nor is it the dynamical variable coupled directly to the oscillator coordinates. Its low-frequency components arise from barrier crossings, the higher ones from oscillations within one valley, to some extent. However,

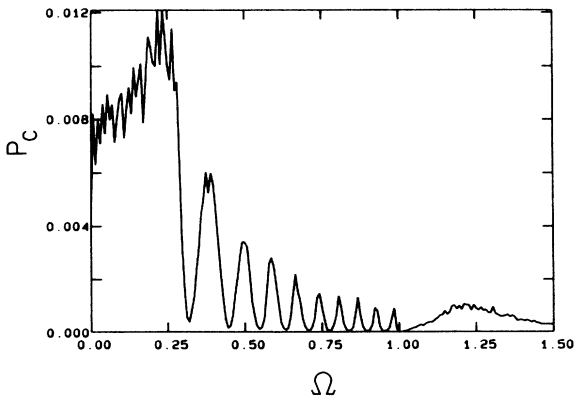

FIG. 7. Power spectra for $\sin(\theta/2)$ with $\alpha=1$, $\mu=1$, and $T^*=1$, and for a 2D Debye density of 10 oscillators.

there is a strong influence due to the bath density of states at all frequencies. Finally, we note that equipartitioning has not been a problem with the rotor, in contrast to the oscillator,[13] suggesting that the nonlinear coupling may be sufficient to bring the rotor to thermal equilibrium, even when the rotor spectral density is nonzero for $\Omega > 1$, the highest bath frequency.

VII. COMPARISON WITH MORI THEORY

In Fig. 8 we exhibit the results of the two schemes (see Sec. III) of the Mori theory for the parameter values $\alpha=0.5$, $\mu=1$, and $T=0.5$, to be compared with Fig. 5. The results for this case give a fair representation of the general situation. The first scheme [Eq. (3.20)] generally gives greater width and less features than the second [Eq. (3.21)]. In this respect the second one is closer to the molecular-dynamics results. The velocity is flat near zero frequency (a Lorentzian central peak), which does not agree with the MD results, in general.[16] The high-frequency peaks in both schemes are at frequencies less than 1, in contrast to the MD results given in Fig. 5. For the sine power spectrum, MD invariably gives a high-frequency peak above unity, which is never the case in either Mori scheme. Mori theory gives a broad central peak for P_s which is absent in the MD results. There is nothing remarkable about the cosine power spectrum, at least in this case, where both Mori theory and MD give narrow central peaks. We conclude that the Mori schemes, at least to this order of approximation, are quite poor, and hence, are not reliable.

VIII. COMPARISON WITH EXPERIMENT

We are aware of only few data with which comparison can be made. Callender and Pershan[5] measured Raman scattering from CN^- impurities in KCl, KBr, and NaCl. They have also studied OH^- and OD^- impurities in these hosts, although for these impurities the classical dynamics approximation may not be justified. The rotational dynamic correlations of T_{2g} symmetry in the case of CN^- impurities in KCl and KBr show a central peak, as our cosine power spectrum does for $\alpha < 1$. The E_g symmetry, on the other hand, shows a single peak at some nonzero frequency. Our simulations show a single finite-frequency peak for one symmetry and a central peak for the other symmetry in the presence of weak rotational-translational coupling, as long as the temperature is less than the adiabatic potential barrier. To see if this behavior persists in the intermediate- to strong-coupling limit ($0.5 < \alpha < 1$), we have run MD simulations for $\alpha=0.75$ and $T=0.1$ and 0.25. In this case, again one sees a behavior qualitatively similar to the weak-coupling results, but only for the sine and cosine power spectra, although the peak positions and widths depend strongly on α. However, the velocity-power spectrum is drastically different in the strong- and weak-coupling limits. From this we conclude that if one is only probing the sine and cosine power spectra, as is done in the Raman scattering experiment, it is not possible from a qualitative analysis of the spectra to differentiate between the low-rigid-barrier weak-coupling limit and the low-adiabatic-barrier strong-

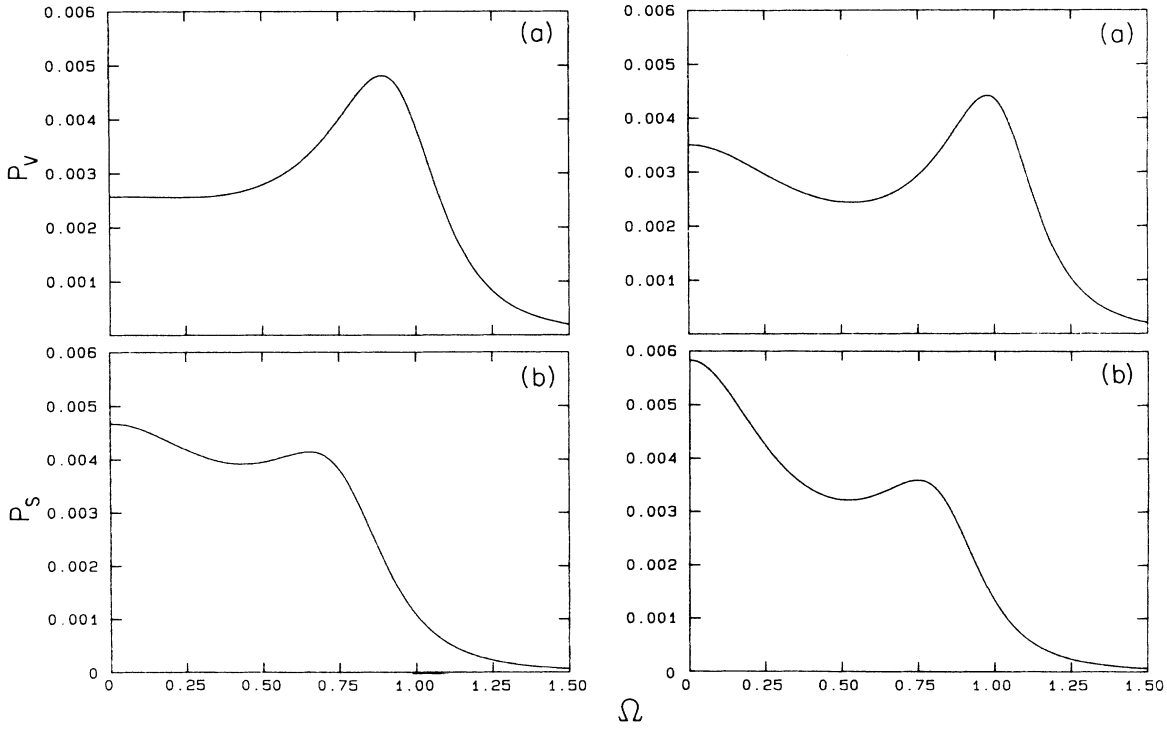

FIG. 8. Power spectra for $\dot{\theta}$ and for $\sin(\theta/2)$ with $\alpha=0.5$, $\mu=1.0$, and $T^*=0.5$ for the first (RM, left-hand panel) and second (MK, right-hand panel) schemes.

coupling limit. One needs to probe the velocity-power spectrum to distinguish between these two fundamentally different limits.

In addition, it would be desirable to have more experimental data, particularly for $\mu \leq 1$, so that two-peak structure could be observed for P_s. Also, to make the model we have studied more realistic, it would be best to have physical systems where the molecular rotation is confined to one angle, as we have done above.

ACKNOWLEDGMENT

This work was partially supported by the National Science Foundation under Grant No. DMR-81-17297.

[1]S. D. Mahanti, P. Murray, and G. Kemeny, Phys. Rev. B **32**, 3263 (1985), and references therein.

[2]Unlike their 3D counterparts, careful experiments on molecular impurities in 2D systems such as $(N_2,O_2)_xAr_{1-x}(x\rightarrow 0)$ have not yet been made.

[3]D. Sahu and S. D. Mahanti, Phys. Rev. B **26**, 2981 (1982). In these ionic solids, such as CN^{-1}, O_2^- in KBr, etc., the potential-energy minimum and the barrier heights depend on short-range repulsion and interaction between the multipole moments of the molecular ion and the surrounding ionic cage. For a rigid lattice, the potential-energy barriers, barring accidental cancellation effects, are usually $\sim 300-500$ K.

[4]F. Lüty, in *Defects in Insulating Crystals,* proceedings of the International Conference on Defects in Insulating Crystals, Riga, 1981, edited by V. M. Turkevich and K. K. Svarts (Springer, Berlin, 1981), pp. 69–89.

[5]R. Callender and P. S. Pershan, Phys. Rev. A **2**, 672 (1970).

[6]This so-called self-energy contribution to the single-site cubic potential depends on the rotational-translation coupling and can significantly modify the single-site potential (see Ref. 1); see also K. H. Michel and J. M. Rowe, J. Chim. Phys. **82**, 199 (1985).

[7]S. D. Mahanti and G. Kemeny, Phys. Rev. B **30**, 7362 (1984).

[8]B. de Raedt and H. de Raedt, Phys. Rev. B **15**, 5379 (1977).

[9]B. de Raedt and K. Michel, Discuss. Faraday Soc. **69**, 88 (1980).

[10]B. de Raedt and K. Michel, Phys. Rev. B **19**, 767 (1979).

[11]G. Kemeny and S. D. Mahanti, Bull. Am. Phys. Soc. **30**, 320 (1985).

[12]G. R. W. Gerling and B. de Raedt, J. Chem. Phys. **77**, 6263 (1982).

[13]G. Kemeny, S. D. Mahanti, and T. A. Kaplan, Phys. Rev. B **34**, 6288 (1986).

[14]G. Kemeny, S. D. Mahanti, and J. M. Gales, Phys. Rev. B **33**, 3512 (1986).

[15]J. Schwinger, J. Math. Phys. **2**, 407 (1961).

[16]If we choose a 1D-oscillator density of states, the central peak becomes extremely flat in the frequency region $0<\Omega<1$, agreeing with the Mori-theory result in the region $\Omega \lesssim 0.6$.